♣ISCCP-FD's Surface Radiation Flux Dataset: Characteristics and Comparison with GEWEX SRB

Yuanchong Zhang[1], William B. Rossow[2] and Paul W. Stackhouse Jr.[3]

[1]*Department of Applied Physics and Applied Mathematics, Columbia University, New York, NY, USA*
[2]*NASA Goddard Institute for Space Studies, New York, NY, USA*
[3]*Atmospheric Science Division, NASA Langley Research Center, Hampton, VA,,USA*

Abstract. Two decades-long global surface radiative flux products, ISCCP-FD and GEWEX/SRB, have been characterized and their 85-89 annual means are compared. Although their global-mean values agree quite well, their regional differences are larger, reflecting differences in their input datasets and radiative transfer treatments, mainly for surface albedo, aerosols and clouds for SW and temperature/humidity profiles and surface skin temperature for LW, respectively. Studying and resolving these differences are necessary to further improve surface radiation budget estimates so that the long-term climate trend may be derived in the future.

Key Words: Surface radiation budget (SRB), ISCCP-FD, GEWEX/SRB, radiative transfer model.

1. INTRODUCTION

Radiation is the primary forcing that drives the weather and climate within the Earth-atmosphere system. Since *Simpson* (1929), estimating Earth's radiation budget has long been pursued. But it is only the advent of satellites that has made it feasible to produce global radiation budget at top of the atmosphere (TOA) and various datasets measuring the physical properties of the atmosphere, clouds and surface that can be put into a radiative transfer model to calculate the radiation budget at the surface (SRF), TOA, and in the atmosphere (ATM). Such calculations are also essential for numerical modeling of the weather and climate. In the past two decades or so, numerous authors have produced satellite-based radiative flux datasets at TOA/SRF; but only recently have there appeared global, decades-long radiative flux datasets produced using more sophisticated radiative transfer models and improved input datasets. Among them are the two flux products from ISCCP-FD (International Satellite Cloud Climatology Project Flux product using the ISCCP D-series data) and GEWEX/SRB (Global Energy and Water Cycle Experiment Surface Radiation Budget project).

2. ISCCP-FD PRODUCT

ISCCP-FD is a self-consistent and integrated radiative flux profile (PRF) product. It contains radiative flux profiles defined by fluxes at five levels: SRF, 680 mb, 440 mb, 100 mb and TOA, and the input atmospheric and surface physical quantities used to calculate them. All of this information is collected into four datasets: FD-TOA, FD-SRF, FD-PRF and FD-INP, where FD-INP is a complete input dataset with virtually all the parameters used in the flux calculation. There is also an additional fifth monthly-mean FD-PRF dataset. Table 1 shows the definition of the five datasets of the ISCCP-FD product.

The FD product has complete global coverage with a spatial resolution of 280 km and time interval of 3-hour and monthly. At the time of writing, it covers a time period from July 1983 to June 2001 but will soon be extended to 2004.

The version of the radiative transfer model used in the flux calculation is 2001 NASA Goddard Institute for Space Studies (GISS) model. The most important characteristics of the

♣ Extended abstract presented at CEReS International Symposium on Radiation Budget and Atmospheric Parameters Studied by Satellite and Ground Observation Data Toward the Understanding of Long Term Trend in Asia, February 17 (Thur.) & 18 (Fri.), 2005, Chiba, Japan.

Table 1. Five Datasets of the ISCCP-FD Product

	Dataset Name	Definition
A	FD-TOA	All the radiative flux components at TOA[a]
B	FD-SRF	All the radiative flux components at SRF[a]
C	FD-PRF	All the radiative flux components for PRF (TOA and SRF, inclusive) [a]
D	FD-INP	Complete input variables used in flux calculation
E	FD-MPF	Radiatively linearly averaged monthly-mean FD-PRF

[a]Including summary of the most important input variables for it.

new GISS model are: (1) higher spectral resolution employing 15 non-contiguous correlated k-intervals to model overlapping cloud-aerosol and gaseous absorption for the shortwave (SW) (nominally 0.2-5.0 :m) with UVA and UVB treatment incorporated; (2) 33 non-contiguous correlated k-intervals for the longwave (LW) (nominally 5.0-200.0 :m, including one for a "window" wavelength: 11.1-11.3 :m) to match line-by-line fluxes to within 1 $Wm^{!2}$ and provide a significant improvement for upper stratospheric cooling rates due to water vapor over the old 1983 GISS model [*Oinas et al*., 2001]; (3) improved surface visible albedo (0.2-0.7 :m) values and a more precise 5-band near-infrared (NIR: 0.7-5.0 :m) albedo representation for 11 "vegetation" type; (4) more comprehensive set of atmospheric gaseous absorbers and aerosols with realistic spatio-temporal variations; (5) explicit treatments of non-spherical ice cloud microphysics and cloud macro-inhomogeneity; (6) realistic non-unit spectral emissivities for surface and cloud LW emission.

With the model, the 5-level downwelling and upwelling SW and LW radiative flux profiles are calculated using the following datasets to specify the properties of the Earth's atmosphere and surface: ISCCP-D1 (*Rossow and Schiffer,* 1999) cloud dataset with a statistical cloud vertical structure (CVS) model, the TIROS Operational Vertical Sounder (TOVS) temperature/humidity profile products, the Total Ozone Mapping Spectrometer (TOMS) ozone products, a climatology of near-surface air temperature (and surface skin temperature) diurnal cycle constructed from NOAA National Weather Service National Meteorological Center (NMC) surface weather reports and the first NCEP reanalysis, a climatology of cloud particle sizes from *Han et al.* (1994), and a climatology of stratospheric and upper tropospheric water vapor and stratospheric aerosols from Stratospheric Aerosol and Gas Experiment II (SAGE-II), a climatology of tropospheric aerosols used in the current NASA GISS climate model.

The complete description of the model, input data, and the sensitivity-study/validation results for FD product may be referred to *Zhang et al.* (2004). The information to obtain the datasets can be found at the ISCCP website (http://isccp.giss.nasa.gov/projects/flux.html),

3. ISCCP FD-SRF DATASET

As the bottom boundary part of the integrated FD flux profiles, the FD-SRF dataset has all the characteristics described above. In *Zhang et al.* (2004), we have repeated virtually all the validation studies for FD-SRF that were done for FD's precursor FC (C for ISCCP C-series data, the precursor of D-series) (*Zhang et al.,* 1995). Overall, FD decreases uncertainties about 5 $Wm^{!2}$ over FC. In addition, we have validated FD using new and more accurate ground 'truth' from the Baseline Surface Radiation Network (BSRN). The BSRN started operations in 1992 with 9 stations and has 35 sites currently. The original target accuracies for BSRN were ±10 $Wm^{!2}$ for downwelling SRF SW ($S9_s$) and ±20 $Wm^{!2}$ for downwelling SRF LW ($L9_s$). But significant improvements in procedures, instrument calibration and knowledge have led to estimated accuracies of ±5 $Wm^{!2}$ for $S9_s$ and ±10 $Wm^{!2}$ for $L9_s$ (*Ohmura et al.,* 1998). The comparisons of monthly, regional mean values from

FD with BSRN values suggests that we have been able to reduce the overall uncertainties to 10-15 W/m^2 at SRF from 20-25 W/m^2 for FC (*Zhang et al.,* 2004).

Table 2a summarizes the statistics of the comparison of all the available and matched, monthly mean FD and BSRN values, totaling 1970 and 1831 data points for $S9_s$ and $L9_s$, respectively. For $S9_s$, the mean (rms) difference (FD ! BSRN) is 2.0 (18.5) Wm$^{!2}$ and the correlation coefficient between the two sets is 0.98. For $L9_s$, these statistics are 2.2 (19.0) Wm$^{!2}$ and 0.97, respectively. Tables 2b and 2c show the same comparison statistics but for seven separate latitudinal zones. For the SW, most zones exhibit differences # 10 Wm$^{!2}$; the largest mean differences appear in the tropical zone (21.3 Wm$^{!2}$), where biomass burning aerosol effects have not been (completely) accounted for in our calculations, and at southern high latitudes (-20.0 Wm$^{!2}$), where the sample size at the surface is very small (23). The largest rms differences appear in the southern and northern polar regions (20.6 and 21.8 Wm$^{!2}$, respectively) with the rest of the zones exhibiting values # 16 Wm$^{!2}$. The correlation coefficients in all zones are above 0.97 except in the tropical zone (0.89). For the LW, all the zones have mean differences # 10 Wm$^{!2}$, except at southern high latitudes (18.8 Wm$^{!2}$) where the sample size is very small. Generally, the LW flux rms differences are slightly larger than for the SW and the correlation coefficients are lower, but still ∃ 0.81, except again at southern high latitudes.

Table 2a. SRF Downwelling SW and LW Fluxes for all FD-SRF and BSRN data♦

Quantity	FD	BRSN	mean difference	Stdv	corr coefficient	Slope	intercept	Norm dev	sample #
$S9_s$	168.20	166.19	2.017	18.491	0.9825	0.96	3.90	13.07	1970
$L9_s$	302.23	300.01	2.219	19.042	0.9706	1.05	-17.40	12.89	1831

Table 2b. SRF Downwelling SW from FD-SRF and BSRN Separated into Latitudinal Zones♦

Lat. Zone	FD	BRSN	mean difference	Stdv	corr coefficient	Slope	intercept	Norm dev	sample #
90E S 6 65E S	114.23	122.36	-8.133	20.599	0.9907	1.05	2.31	13.38	302
65E S 6 35E S	145.18	165.15	-19.972	15.370	0.9822	1.03	15.08	10.53	23
35E S 6 15E S	217.11	219.53	-2.412	11.728	0.9847	1.00	2.32	8.29	144
15E S 6 15E N	247.72	226.40	21.318	13.963	0.8928	0.95	-9.03	10.07	218
15E N 6 35E N	210.87	200.61	10.262	16.092	0.9742	0.97	-4.65	11.45	243
35E N 6 65E N	168.34	168.23	0.116	14.180	0.9847	0.95	7.96	9.88	819
65E N 6 90E N	86.64	86.63	0.005	21.798	0.9724	0.97	3.01	15.51	221

Table 2c. SRF Downwelling LW between Latitudinal-zonal FD-SRF and BSRN♦

Lat. Zone	FD	BRSN	mean difference	Stdv	corr coefficient	Slope	intercept	Norm dev	sample #
90E S 6 65E S	194.11	184.12	9.994	19.127	0.9478	1.14	-36.49	11.90	276
65E S 6 35E S	316.67	297.85	18.820	17.132	0.2916	0.60	107.75	14.40	23
35E S 6 15E S	357.99	360.82	-2.828	22.663	0.8122	1.09	-30.75	15.18	141
15E S 6 15E N	414.65	415.33	-0.680	8.797	0.8094	0.80	84.20	6.49	136
15E N 6 35E N	360.45	356.36	4.096	19.956	0.8634	1.00	-4.25	14.11	237
35E N 6 65E N	305.72	307.05	-1.327	17.688	0.9209	0.98	7.50	12.62	814
65E N 6 90E N	251.83	244.61	7.217	20.080	0.9293	1.33	-91.49	10.18	204

♦Regression statistics are from a linear least squares fit to the scatter of points, X/Y for FD-SRF/BSRN. All values are in Wm$^{!2}$, except the correlation coefficients and slopes, which are unitless. "Norm Dev" is the rms distance of all the points from the regression line.

4. GEWEX SRB DATASET

GEWEX-SRB (Release 2) dataset is also a global, long-term set with a higher spatial resolution of 1º X 1º at 3-hour temporal interval. It covers a time period of 12 years (July 1983 - October 1995) (*Stackhouse et al.,* 2001, 2004) but will soon be extended to 2004. Its

radiative transfer algorithms are from *Pinker and Laszlo* (1992) and *Fu et al.* (1997) for broadband SW (0.2-4.0 :m) and LW (4.5-∞ :m), respectively. Among the input datasets, cloud information is from ISCCP-DX (*Rossow et al.,* 1996), the atmospheric temperature/humidity profiles are from the Goddard Earth Observing System (version1, GEOS-1) reanalysis, surface skin temperature is from GEOS-1 (originally from *Reynolds,* 1988) over oceans and land with more than 50% cloud cover and from ISCCP for land with less than 50% cloud cover and snow/ice covered surfaces. Ozone data is from TOMS integrated with TOVS when needed. The surface albedo is obtained from Pinker/Laszlo algorithm (*Pinker and Laszlo,* 1992) and the emissivity map is adapted from the CERES-SARB surface emissivity map (*Wilbur et al.,* 1999). A background aerosol is assumed based upon surface type in the Pinker/Laszlo model adapted from the *WCP-55* (1983) aerosol types. The effective optical depths are scaled in the algorithm to account for differences between composite clear-sky and observed clear radiances. The monthly averaged mean (RMS) difference of GEWEX SRB compared against all BSRN site measurements from 1992 – 1995 is -3.4 (23) Wm^{-2} for SW fluxes and –5.2 (15.5) Wm^{-2} for LW fluxes, respectively. That exclusion of polar sites reduces SW monthly mean (rms) difference to –0.2 (18.5) Wm^{-2} indicates a need for further study in the polar regions (*Stackhouse, et al.,* 2004).

5. SURFACE FLUX COMPARISON BETWEEN FD-SRF AND SRB

Table 3 shows statistical results from the comparison between FD-SRF and SRB for global averages of all the primary and derived surface flux components based on 5-year (85-89) annual means (with SRB map regridded to ISCCP's standard 280-km equal-area map).

Table 3. Comparison of Global Mean for 85-89 Annual Mean between FD-SRF and SRB †

Quantity	FD	SRB	mean diff.	STDV.	Cor.Coef.	SLOPE	Intercept	norm dev	Cell #
$S\downarrow_s$	189.2	186.9	2.34	10.50	0.9832	1.007	-3.69	7.39	6596
$S\uparrow_s$	24.0	21.8	2.21	7.01	0.9542	0.812	2.30	4.38	6596
ALB_s	15.0	13.9	1.13	3.47	0.9846	0.876	0.74	2.04	6596
CLR-$S\downarrow_s$	248.3	244.3	3.98	11.76	0.9766	0.990	-1.39	8.35	6596
CLR-$S\uparrow_s$	29.8	28.6	1.22	7.96	0.9571	0.826	3.96	5.04	6596
CLR-ALB_s	14.3	14.1	0.25	3.15	0.9843	0.907	1.07	2.03	6596
NS_s	165.2	165.1	0.13	9.91	0.9876	0.976	3.86	7.01	6596
CLR-NS_s	218.5	215.7	2.76	13.12	0.9821	0.964	5.17	9.27	6596
$L\downarrow_s$	344.7	343.2	1.49	10.16	0.9894	1.035	-13.69	6.88	6596
$L\uparrow_s$	395.6	393.7	1.90	11.15	0.9889	0.980	6.19	7.89	6596
CLR-$L\downarrow_s$	313.6	306.2	7.43	11.30	0.9888	1.002	-8.16	7.98	6596
CLR-$L\uparrow_s$	394.1	393.2	0.96	11.26	0.9888	0.973	9.81	7.94	6596
NL_s	-50.9	-50.5	-0.40	13.04	0.7878	0.733	-13.17	9.53	6596
CLR-NL_s	-80.5	-87.0	6.48	13.38	0.7230	0.823	-20.73	10.08	6596
N_s	114.3	114.6	-0.28	16.48	0.9612	1.041	-4.42	11.31	6596
CLR-N_s	137.9	128.7	9.24	19.93	0.9623	0.987	-7.42	14.17	6596
CFC-NS_s	-53.3	-50.6	-2.63	6.55	0.9544	0.942	-0.45	4.68	6596
CFC-NL_s	29.6	36.5	-6.88	3.95	0.9515	0.929	8.98	2.82	6596
CFC-N_s	-23.7	-14.2	-9.51	7.56	0.9356	0.902	7.19	5.39	6596

† In addition to the symbols/acronyms similar to those in Table 2 (X/Y for FD/SRB now), CLR=clear-sky, CFC=cloud flux change ("cloud forcing"), ALB=albedo, N=net, and ↑ is for those upwelling fluxes.

Generally speaking, the two's agree reasonably well: for all the primary flux components (i.e., $S\downarrow_s$, $S\uparrow_s$, $L\downarrow_s$ and $L\uparrow_s$ and their clear-sky counterparts, see footnotes in Table 3 for symbol definitions), their mean differences are < 4 Wm^{-2} (except CLR-$L\downarrow_s$) with rms < 12 Wm^{-2}, and their spatial correlation coefficients are > 0.95.

However, regional differences are evident and there seem to be some systematic patterns associated with specific meteorological, cloud and aerosol conditions in some regions. Figure 1 shows global difference maps of $S\downarrow_s$, $S\uparrow_s$, CLR-$S\downarrow_s$ and CLR-$S\uparrow_s$, respectively. The three big yellow circular patterns in CLR-$S\uparrow_s$ map are obviously related to view angle of individual geostationary satellites, primarily from the surface albedo retrieval

method of SRB. Comparing CLR-S$\downarrow_s$ and CLR-S$\uparrow_s$ maps shows FD has lower surface albedo than SRB in most of the northern part of South America and the southern part of Africa. In the polar regions, FD has generally higher surface albedo than SRB. There is an area in

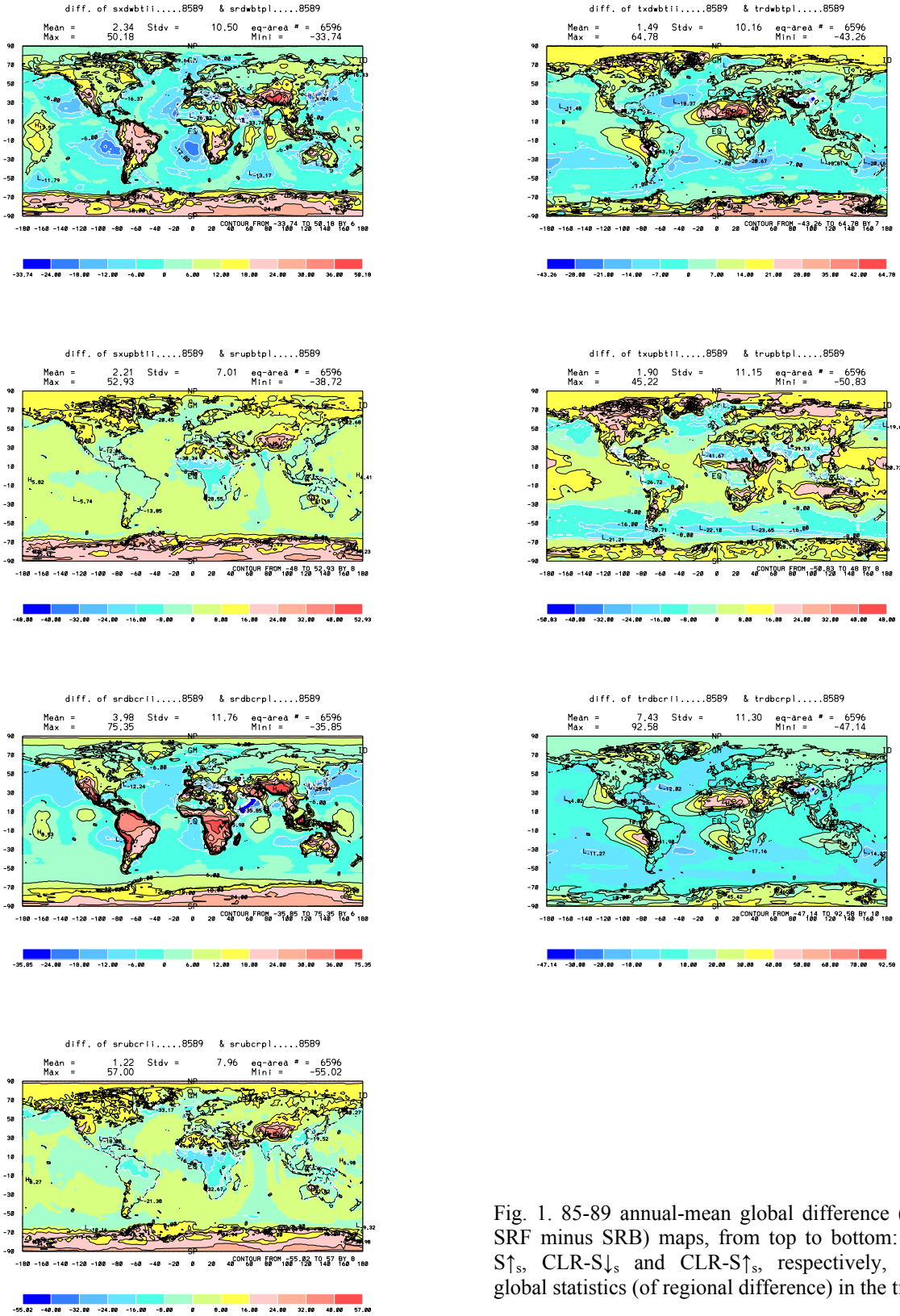

Fig. 1. 85-89 annual-mean global difference (FD-SRF minus SRB) maps, from top to bottom: S$\downarrow_s$, S$\uparrow_s$, CLR-S$\downarrow_s$ and CLR-S$\uparrow_s$, respectively, with global statistics (of regional difference) in the titles.

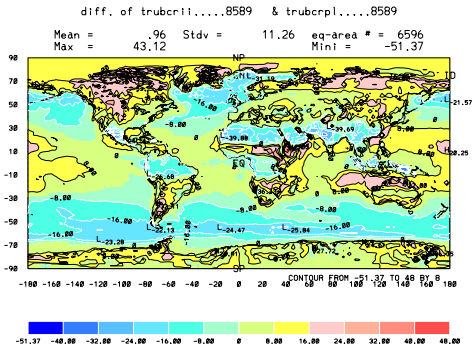

Fig. 2. 85-89 annual-mean global difference (FD-SRF minus SRB) maps, from top to bottom: $L\downarrow_s$, $L\uparrow_s$, CLR-$L\downarrow_s$ and CLR-$L\uparrow_s$, respectively, with global statistics (of regional difference) in the titles.

central China where FD has up to > 40 Wm^{-2} higher SW than SRB (for both CLR-$S\downarrow_s$ and CLR-$S\uparrow_s$). This is because FD's aerosols are much less than SRB in that area, where FD's absorbed atmospheric SW is up to 30 Wm^{-2} less than SRB (not shown). In the top panel ($S\downarrow_s$) of Fig. 1, there are several oceanic areas (two in the eastern Pacific, two in the eastern Atlantic, and one in the northwestern Pacific) where FD is as much as 18 Wm^{-2} less than SRB, likely caused by two different treatments of clouds: although both data products draw their cloud-related information from ISCCP, the FD product uses all of the cloud properties reported by ISCCP whereas SRB uses only cloud cover and visible reflectance. Figure 2 shows the LW counterparts of Fig. 1. The first and third panels ($L\downarrow_s$ and CLR-$L\downarrow_s$) suggest that there are some fundamental differences (with a global mean difference > 7 Wm^{-2} for CLR-$L\downarrow_s$) in the input temperature/humidity profiles from TOVS and GEOS-1 that the most of the larger differences of FD's values in west coast areas in eastern Pacific and Atlantic oceans and the belt from northern Africa to mid-east areas but a reverse difference in central-western China. Such large systematic differences need further study. The upwelling LW (panels 2 and 4 in Fig. 2) differences are primarily caused by different input surface skin temperature data sets: for ocean area and land areas with > 50% cloud cover, it reflects the differences between ISCCP and Reynolds, and for the rest land areas, it reflects FD's diurnal adjustment (*Zhang et al.,* 2004) that makes its surface skin temperature different from the original ISCCP's.

6. CONCLUSIONS

Two decades-long global surface radaitive flux data products are introduced and their 85-89 annual means are compared. Although their global mean values agree reasonably well, there are regional differences that require further investigation. The main comparable causes are likely the two's different input datasets and treatments for surface albedo, aerosols and clouds for SW, and temperature/humidity profiles and surface skin temperature for LW. Nevertheless, the overall agreement of these two products, to within 10-20 Wm^{-2}, indicates that they both can be usefully applied to study the factors controlling the weather-scale variations of surface fluxes. Resolution of some of the differences will allow these data products to be used to study interannual variations as well.

7. REFERENCES

Fu. Q., K.-N. Liou and A. Grossman, 1997, Multiple scattering parameterization in thermal infrared radiative transfer, *J. Atmos. Sci., 54,* 2799-2812.

Han, Q., W.B. Rossow, and A.A. Lacis (1994), Near-global survey of effective droplet radii in liquid water clouds using ISCCP data, *J. Climate, 7,* No. 4, 465-497.

Ohmura, A., E.G. Dutton, B. Forgan, C. Fröhlich, H. Gilgen, H. Hegner, A. Heimo, G. König-Langlo, B. McArthur, G. Müller, R. Philipona, R. Pinker, C.H. Whitlock, K. Dehne, and M. Wild (1998), Baseline surface radiation network (BSRN/WCRP): new precision radiometry for climate research, *Bull. Amer. Meteor. Soc., 79,* No. 10, 2115-2136.

Oinas, V., A.A. Lacis, D. Rind, D.T. Shindell and J.E. Hansen (2001), Radiative cooling by stratospheric water vapor: Big differences in GCM results, *Geophys. Res. Lett., 28*, 2791-2794.

Pinker, R.T. and I. Laszlo (1992), Modeling surface solar irradiance for satellite applications on global scale, *J. Appl. Meteor., 31,* 194-211.

Reynolds, C.D. (1988), A real time global sea surface temperature analisys, *J. Climate, 1,* 75-86.

Rossow, W.B., A.W. Walker, D.E. Beuschel and M.D. Roiter (1996), *International Satellite Cloud Climatology Project (ISCCP) documentation of new cloud datasets,* WMO/TD-No. 737, World Climate Research Programme (ICSU and WMO), 115 pp.

Rossow, W.B. and R.A. Schiffer (1999), Advances in understanding clouds from ISCCP, *Bull. Amer.Meteor. Soc., 80,* 2261-2287.

Simpson, G.C. (1929): The distribution of terrestrial radiation. *Mem. Roy. Meteor. Soc., 3,* 53-78.

Stackhouse Jr., P.W., Stephen J. Cox, Shashi K. Gupta, Marc Chiacchio, and J. Colleen, Mikovitz (2001), The WCRP/GEWEX surface radiation budget project release 2: An assessment of surface fluxes at 1 degree resolution. International Radiation Sysposium, St.-Petersburg, Russia, July 24-29, 2000. *IRS 2000: Current Problems in Atmospheric Radiation,* W.L. Smith and Y. Timofeyev (eds.), A. Deepak Publishing, 147.

Stackhouse Jr., P.W., S.K. Gupta, S.J. Cox, J.C. Mikovitz, T. Zhang, and M. Chiacchio, and (2004), 12-Year Surface Radiation Budget Data Set, *GEWEX News,* November,10-12.

WCP-55 (1983). *World Climate Research Report of the experts meeting on aerosols and their climatic effects,* Williamsburg, Virginia, 28-30 March 1983, Eds: A. Deepak and H. E. Gerber, 107 pp.

Wilber, A. C., D. P. Kratz, S. K. Gupta, 1999: *Surface emissivity maps for use in satellite retrievals of Longwave Radiation*, NASA Technical Publication, 1999-209362*,* 35 pp.

Zhang, Y.-C., W.B. Rossow and A. A. Lacis (1995), Calculationof surface and top of atmosphere radiative fluxes from physical quantities based on ISCCP data sets, 1. Method and sensitivity to input data uncertainties, *J. Geophys. Res., 100,* 1149-1165.

Zhang, Y-C., W.B. Rossow, A.A. Lacis, V. Oinas and M.I. Mishchenko (2004), Calculation of radiative fluxes from the surface to top-of-atmosphere based on ISCCP and other global datasets: Refinements of the radiative transfer model and the input data, *J. Geophys. Res., 109,* D19105, doi:10.1029/2003JD004457.